Combining Machine Learning and Spatiotemporal Filtering to Map Crop Types of Germany for Seven Years

Ursula Gessner, Andreas Hirner, Sarah Asam, Martina Wenzl, and Claudia Kuenzer

***Abstract*—Knowledge of the distribution of crop types and their sequence over the years is essential not only for scientific applications but also for supporting informed planning for food security, climate adaptation and mitigation, agroecology, and landscape diversity. For Germany, crop type information is collected as part of the subsidy management, but data access is restricted for certain years and Federal States. Remote sensing time series of sensors, such as Sentinel-1 and Sentinel-2, allows national mapping of crop types at field scale. This has been demonstrated in previous literature, which describe crop type mapping of Germany for one to three years. Here, we demonstrate a two-phase crop type classification methodology based on Sentinel-1 and Sentinel-2 data. The approach combines machine learning (ML)-based classification with spatial and temporal analyses. The methodology was used to create a novel and most recent seven-year time series (2018–2024) for Germany at 10-m spatial resolution separating 18 classes. The two-phase approach led to annual overall accuracies (OAs) of 0.81–0.83 with average class-specific *F*1-scores ranging from around 0.56–0.99.**

***Index Terms*—Agriculture, Central Europe, cropland, grassland, integrated administration and control system (IACS), random forest (RF), time series.**

I. Introduction

THE knowledge of which crop types are cultivated where and when provides fundamental information for many applications in the context of climate change adaptation, food security, agricultural policies, and agroecology. Data on crop types are collected within the EU as part of subsidy management, but data access is oftentimes restricted for reasons of confidentiality so that is not possible to obtain continuous information in space and time. Satellite Earth observation (EO) has been well-established for mapping of agricultural land use for many years [1], [2]. It has considerably gained significance since the launch of the Copernicus satellites, which have made it possible to map the land surface with high spatial and temporal resolution. With Sentinel-1 A/B (S-1) and Sentinel-2 A/B (S-2) data that is available jointly since mid-2017, dense (five-day) time series is available at 10–20 m. These time series are uniquely suited for mapping agricultural land use in detail: their high frequency allows to capture the temporal development of crops—which is crucial for differentiating crop types—and they deliver data at field scale. In the past years, machine learning (ML) algorithms have proven to be well-suited for mapping land use, achieving robust and good accuracies at relatively low computational costs, e.g., [3], [4], [5]. In recent years, deep learning approaches have gained increasing attention, particularly for complex settings like small-scale agriculture, or catch crop mapping, e.g., [6], [7], [8]. Many crop type mapping approaches use only multispectral data, e.g., [4], [9], [10] or less frequently-only synthetic aperture radar (SAR) data, e.g., [5], [11], [12]. However, the advantage of using multispectral in combination with SAR time series has been clearly demonstrated for different regions worldwide, e.g., [13], [14], [15], [16], [17], [18]. The German-wide crop type mapping approaches and their respective datasets published in literature cover one [9], [10], [13] to three [3] years only. The underlying methodologies use annual data for mapping individual annual maps. However, with an increasing length of the S-1/2 time series and the data continuation by the newly launched S-1 C, new potential arises to integrate knowledge on interannual crop sequences and typical class confusions for enhancing accuracies and producing stable multiannual maps.

This letter presents a two-phase classification methodology that was used to derive the most up-to-date series of crop type maps of Germany for seven years from S-1 and S-2 data, including a comprehensive validation of the results. The methodology is a further development of [13], where major improvements comprise: 1) the integration of a secondary classification step based on temporal and spatial filtering; 2) the modification of temporal interpolation techniques during data preprocessing, as well as of spectral features; and 3) an adapted set of considered crop types.

II. Methodology

An overview over the methodology is shown in Fig. 1. In the first step of the classification, S-1/S-2 data of 2018–2024

Received 28 February 2025; revised 29 April 2025 and 27 June 2025; accepted 6 July 2025. Date of publication 10 July 2025; date of current version 21 July 2025. This work was supported in part by the German Aerospace Center (DLR) Funds, in part by the Helmholtz Association of German Research Centers under the Helmholtz Climate Initiative (HI-CAM: Helmholtz-Initiative Climate Adaptation and Mitigation); in part by the Federal Ministry of Food and Agriculture through the Project “Einsatz von Fernerkundungstechnologien für die Digitalisierung im Pflanzenbau (AgriSens DEMMIN 4.0)” under Grant 28DE114C18 and Grant 28DE114C22; and in part by The Free State of Bavaria via the Bavarian State Ministry of Economic Affairs, Regional Development and Energy as part of the “Earth Observation Innovation Laboratory for Climate Adaptation and Mitigation” Project (www.EO4CAM.de). *(Corresponding author: Ursula Gessner.)*

The authors are with German Remote Sensing Data Center (DFD), German Aerospace Center (DLR), 82234 Weßling, Germany (e-mail: ursula.gessner@dlr.de; andreas.hirner@dlr.de; sarah.asam@dlr.de; martina.wenzl@dlr.de; claudia.kuenzer@dlr.de).

This article has supplementary downloadable material available at https://doi.org/10.1109/LGRS.2025.3587517, provided by the authors.

Digital Object Identifier 10.1109/LGRS.2025.3587517

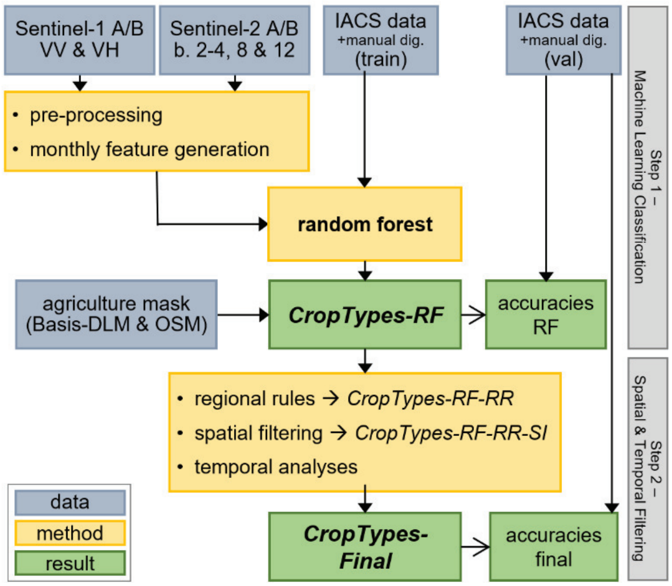

Fig. 1. Overview of the methodological approach.

serve as an input to a random forest (RF) [19] classification. Training of the RF is mainly based on the data of the Integrated Administration and Control System (IACS) for six German Federal States. In the second step, the crop types time series is further improved based on a set of spatial and temporal analyses.

A. Satellite Input Data and Preprocessing

S-1 and S-2 acquisitions taken between March and October 2018–2024 were analyzed. The exclusion of winter months was necessary as they are strongly affected by cloud (S-2) and snow cover (S-1 and S-2). All S-2 data were atmospherically corrected [20], the 20-m bands were resampled to 10 m, and cloudy pixels were excluded based on FMASK [21]. Data of bands 2, 3, 4, 8, and 12 were resampled to equidistant five-day intervals and gaps were filled by temporal linear interpolation. In order to allow gap-filling also at the start (March) and end (October) of the annual time series, auxiliary shoulder datasets were created by first calculating pixel-based mean reflectances per band from all data of February and November, respectively. Remaining gaps were filled by overlaying these mean values with the ESA WorldCover 2020 map [22], and class-wise mean reflectances per band were calculated after outliers were eliminated using the interquartile range. Finally, gaps and outlier pixels were filled by the above calculated band- and class-wise mean reflectance values, according to their ESA WorldCover class. The shoulder datasets were not used as an input to the classification but only as lateral values for the gap-filling procedure described above. The five-day time series was smoothed using the Savitzky and Golay [23] with a window size of 31 days and polynomial order of 2 to reduce remaining noise in the data. Finally, four spectral indices, Normalized Difference Vegetation Index (NDVI), Normalized Difference Yellowness Index (NDYI), Enhanced Vegetation Index (EVI), and Soil-Adjusted Vegetation Index (SAVI), were calculated. Compared to [13], where only NDVI was used, we added SAVI as it was shown to be the most important spectral index in [3] for Germany, by NDYI as we saw potential to increase rapeseed accuracies [24], and by EVI as it is sensitive to biophysical variations even for dense canopies [25] being relevant for late growth stages.

S-1 ground range detected data in descending mode were used for the same months and years as S-2. SAR is a valuable complement of optical data due to its sensitivity to vegetation structure and as it is hardly cloud-affected. The steps to obtain backscatter (VV and VH) included orbit correction, thermal and border noise removal, radiometric calibration, speckle-noise filtering, terrain correction, and conversion to decibel units using the SNAP S-1 toolbox [26]. S-1 data were resampled to the S-2 10-m grid using a nearest neighbor approach and subset to the S-2 tile system. VV and VH were chosen over other S-1 indices as previous studies identified them being most relevant for crop classification in Germany [3].

Per-pixel monthly statistics (arithmetic mean, minimum, and maximum) were finally calculated for the S-2 bands 2–4, 8, and 12, for the spectral indices (NDVI, NDYI, EVI, and SAVI), and for S-1 VV and VH backscatter, resulting in a set of 216 multispectral and 48 SAR features.

B. Reference Data and Classification Scheme

Based on the use types of IACS, 18 classes were defined (Table S1, supplementary). Details on the reasoning behind class definition can be found in [13]. Compared to [13], however, we added "permanent grassland" and amended the class "fruit trees" to "fruit trees and other woody vegetation" (FTWV) to account for woody elements within agricultural areas.

The reference data for building the RF and for validation were taken from anonymized polygon data of the IACS for the Federal States of Mecklenburg-Western Pomerania, Brandenburg, North Rhine-Westphalia, Baden-Wuerttemberg, Hesse, and Lower Saxony. The data were available at an annual basis for all years of the study period, with an exception of 2018 for North Rhine-Westphalia and 2023 and 2024 for Baden-Wuerttemberg. The distribution of the datasets guarantees a broad geographical coverage, representing the range of agricultural landscapes of Germany. As the available IACS data did not contain sufficient hops data in 2023 and 2024, we manually digitized hops fields based on very high-resolution data available in Google Earth Pro [27] and aerial imagery. Before samples were taken, all field polygons were reduced by a buffer of 20 m in order to minimize potential inconsistencies of geolocation or polygon geometry. For each of the 18 classes and for every year, 2000 samples were randomly selected from the IACS of the respective year and from the manually digitized hops data. Equal size sampling per class was applied (similar to, e.g., [3], [13], [24]) in order to avoid a bias of the RF results toward large classes. It has to be considered that this sampling scheme reduces the standard error of user's accuracies but increases those of producer's accuracies [28]. In cases where at least 2000 fields were available per class, the sampling process ensured that only one central sample was taken per field. This was possible for all classes except for hops where multiple samples needed to be taken per field, with a minimum distance of 40 m between samples. The samples were split into a dataset for building the RF and one for validation, each containing 1000 samples per class. During splitting, it was ensured that hops samples from the same field were uniformly kept either for training or for validation.

C. Classification and Spatial/Temporal Filtering

In the first step of the classification procedure, the pixel-based RFs [19] were created (Fig. 1). RFs are established algorithms for classification in EO and were selected here as they are reported to provide good accuracies, robustness with respect to parameter settings, multicollinearity, and overfitting [19], [29] and show relatively low computational complexity, making them suited for operational processing. The RF analysis was implemented using the python "scikit-learn" package version 1.3.1 [30]. RFs were built with 100 trees, and max_features was set to the square root of the total number of features. For each year, an individual RF was constructed based on training data as described in section B and S-1 and S-2 features as described in section A and applied to Germany. RF feature importance values were calculated and summed up for all features of one month and sensor type to assess the relative importance of acquisition time and SAR/optical data. Nonagricultural areas were excluded from the results using Basis-DLM (*Digitales Basis-Landschaftsmodell*) datasets of the German Federal States [31], [32], [33]. From these datasets, the object-type "agriculture" without subgroup "garden land" was used and reduced by the classes "railway, highway, waterway" of OpenStreetMap [34]. Overall accuracies (OAs) and class-specific $F1$-scores were calculated for this intermediate mapping result (*CropTypes-RF*) based on the validation data.

The seven years of *CropTypes-RF* were further improved by spatial and temporal analyses that consist of: 1) regional rules; 2) spatial filtering; and 3) temporal analyses (Fig. 1) as follows. In Germany, the cultivation of hops and wine is restricted to certain broader regions. As the intermediate *CropTypes-RF* showed a certain overestimation of vineyards and hops outside these areas, a reclassification was conducted. Thus, the potential hops and wine growing regions were defined based on the Basis-DLM datasets, where the polygons of the classes "Hopfen" (hops) and "Weingarten" (vineyard) were enlarged by a buffer of 10 km. In case hops and vineyard pixels were located outside these defined growing areas, they were assigned to a new class "other agricultural use." In contrast, vineyard and hops pixels in the high mountain areas of the Alps ("Alpen," according to [35]) were reclassified to "permanent grassland," as we identified consistent confusion between vineyards/hops and grassland for this area. The intermediate map that resulted from this regional rule processing step is called *CropTypes-RF-RR* in the following.

Subsequently, group-wise spatial filters were applied to eliminate smaller patches (<0.4 ha) of misclassifications that sometimes occur between spectrally and/or phenologically similar classes. Based on the confusion matrices of *CropTypes-RF*, four groups of frequently confused classes were identified: 1) winter wheat, winter barley, winter rye, and other winter cereals; 2) spring wheat, spring barley, and spring oat; 3) legumes, potatoes, and sugar beet; and 4) clover/alfalfa, arable grass, and permanent grassland. In four parallel operations, the pixels classified into one of these groups of classes were kept while all other pixels were set to no-data. Then, a sieve filter removed all contiguous pixels forming patches <0.4 ha, and the resulting gaps were filled with the pixel value of the largest neighboring patch. In case a gap could not be filled due to missing neighboring polygons, the original value of the pixel was kept. Subsequently, the four sieved datasets were merged and no-data values were filled by the pixel values of *CropTypes-RF-RR*. The resulting intermediate map is called *CropTypes-RF-RR-SI*.

Furthermore, the maps were improved based on temporal consistency analysis. A time series of crop types was built from the seven annual *CropTypes-RF-RR-SI* datasets and permanent classes (vineyards, hops, FTWV, and permanent grassland) were inspected. In case a pixel was classified as hops, vineyard, or FTWV in >50% of the years, the complete pixel time series was set to hops, vineyard, or FTWV, respectively. In case a pixel was assigned to hops, vineyards, or FTWV in 50% of the years or less, the respective hops/vineyard/FTWV values were reclassified to "other agricultural use." We found relatively high confusion rates between grassland classes (81, 82, and 83) in *CropTypes-RF*. Specifically, permanent grassland was misclassified as temporal grassland classes in single years. Therefore, we applied a consistency rule to reclassify all pixels that showed grassland classes throughout all years to "permanent grassland" (83).

Finally, a sieve filter was applied to the adapted dataset again to remove patches <0.4 ha that were created during the suite of spatial and temporal analyses. OAs and class-specific $F1$-scores were calculated for the final maps (*CropTypes-Final*) based on the validation sample set.

III. Results

Fig. 2 shows the crop type map *CropTypes-Final* for the year 2024. It depicts the major crop growing regions of Germany well, including the areas dominated by maize in the northwest and southeast, or the *Boerde* areas in central Germany, characterized by a mixture of mainly winter cereals, winter rapeseed, sugar beet, and maize. The results also reflect the spatial diversity of crop patterns with a wide range of parcel shapes and sizes, as shown in Fig. 3. This figure illustrates the level of within-field consistency, which was achieved without including field boundaries. The OAs range between 0.81 and 0.83 for the seven annual maps (Fig. 4). These OAs, and in most cases also class-specific recall and precision values (Figs. S2 and S3, supplementary), are higher than those achieved in other studies [3], [13] that also mapped crop types all over Germany for overlapping years with a uniform classification model and that used IACS data for validation (model OAs: [3] for 2018: 0.77; [3] for 2019: 0.75; [13] for 2018: 0.7). However, it needs to be noted that the accuracy measures are not perfectly comparable due to not identical legends and validation samples.

To identify spatial variations in accuracies for different landscapes, we assessed three natural regions [35] that covered major parts of the validation areas for 2024. This

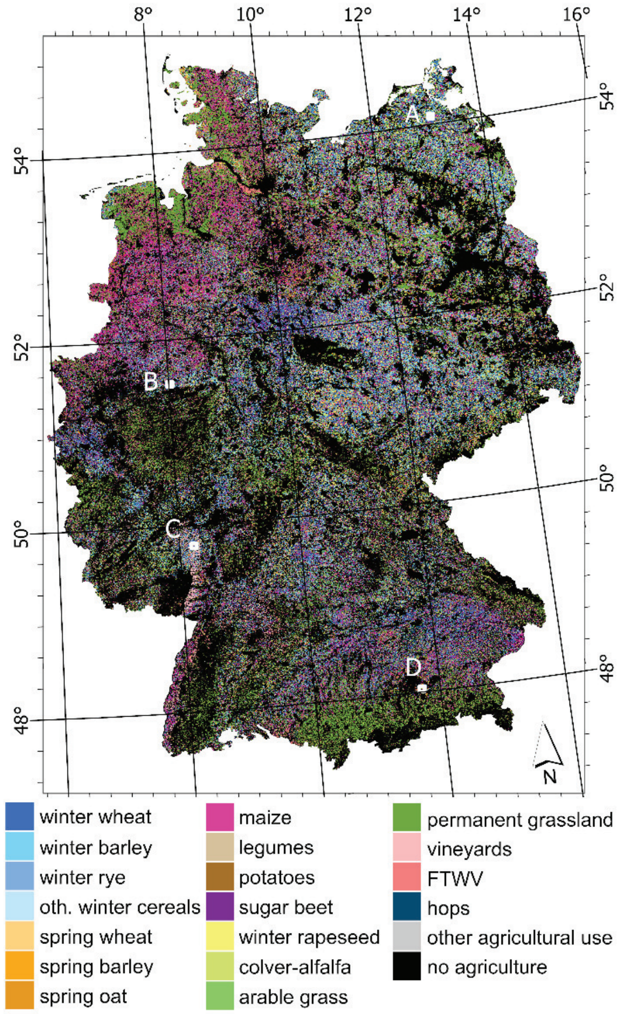

Fig. 2. Crop type map of Germany for the year 2024. White boxes indicate the location of the detailed views of Fig. 3.

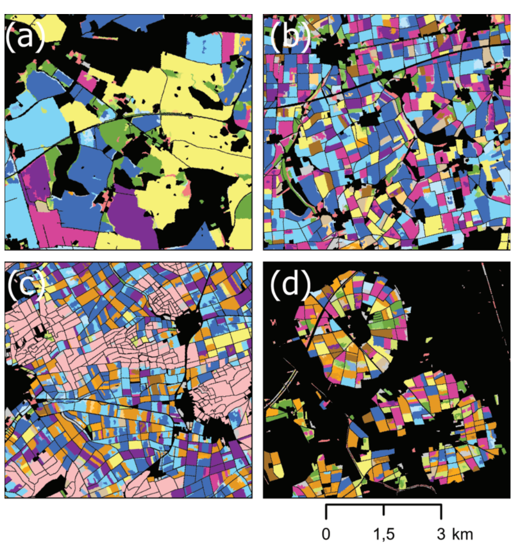

Fig. 3. Detailed view of the crop type map 2024. Location of the regions: see Fig. 2.

analysis showed that accuracies were relatively stable in space ranging between 0.72 (“north-eastern German lowlands”),

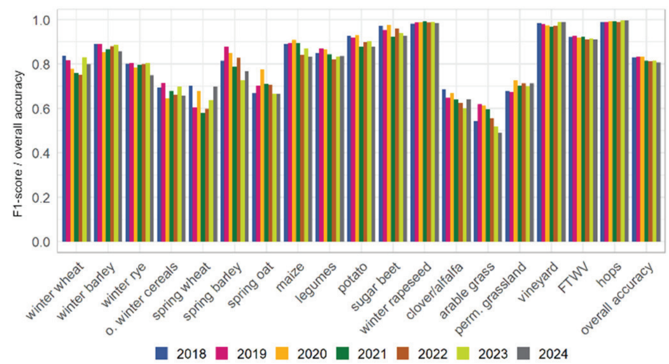

Fig. 4. Overall accuracy and class-specific $F1$-scores of the seven annual crop type maps *CropTypes-Final*.

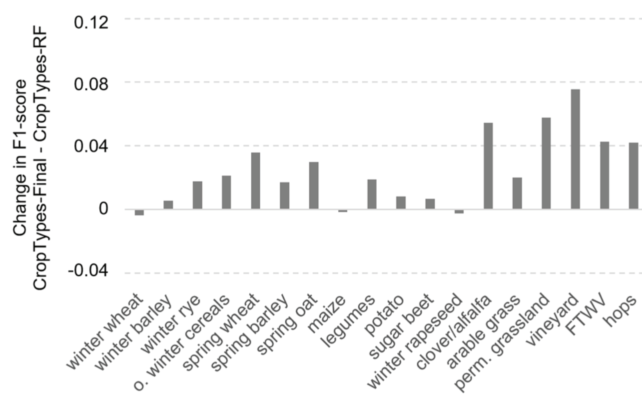

Fig. 5. Mean difference in $F1$-scores between final (*CropTypes-Final*) and intermediate (*CropTypes-RF*) result.

0.81 (“north-western German lowlands”), and 0.78 (“western medium-range mountains”). Highest $F1$-scores (multiannual averages) >0.9 were identified for potato, sugar beet, winter rapeseed, vineyards, FTWV, and hops. Winter barley and maize also showed high average $F1$-scores of 0.87 and 0.88. They are followed by winter wheat, winter rye, spring barley, and legumes ($F1$-scores: 0.79–0.84). For the remaining cereals, clover/alfalfa, and permanent grassland, average $F1$-scores range between 0.64 and 0.7, while lowest accuracies were reached for arable grass (0.56). Confusion matrices giving details on typical class confusions can be found in Figs. S1–S3 (supplementary). The $F1$-scores are relatively stable over the years of analysis with a mean difference between minimum and maximum class-specific $F1$-scores of 0.07.

Comparing the accuracies of the purely ML-based result (*CropTypes-RF*) with the final dataset after additional spatial and temporal filtering (*CropTypes-Final*), we found an increase in $F1$-scores for almost all classes, reaching up to 0.076, except for winter wheat, maize, and winter rapeseed, with a neglectable decrease between −0.002 and −0.004 (Fig. 5).

The top five relevant feature groups were identified to be the S-2 features of August, S-1 features of June, and S-2 features of April, May, and July. This study presents the currently longest scientifically published and validated crop type time series of Germany. Relying on the increasing length of Sentinel time series, annual crop type maps can be clearly improved by integrating knowledge on typical class confusions and interannual crop sequences. The enhanced and stable results can form a valuable basis for further applications, for example, for monitoring landscape diversity, crop rotation, and management. The dataset is available at https://geoservice.dlr.de/web/

ACKNOWLEDGMENT

The authors would like to thank German Federal States for providing Basis-DLM and IACS data and appreciate the provision of OpenStreetMap data copyrighted by OpenStreetMap contributors.

REFERENCES

[1] B. Wu et al., "Challenges and opportunities in remote sensing-based crop monitoring: A review," *Nat. Sci. Rev.*, vol. 10, no. 4, p. 290, Mar. 2023, doi: 10.1093/nsr/nwac290.

[2] M. A. Machichi et al., "Crop mapping using supervised machine learning and deep learning: A systematic literature review," *Int. J. Remote Sens.*, vol. 44, no. 8, pp. 2717–2753, Apr. 2023, doi: 10.1080/01431161.2023.2205984.

[3] L. Blickensdörfer, M. Schwieder, D. Pflugmacher, C. Nendel, S. Erasmi, and P. Hostert, "Mapping of crop types and crop sequences with combined time series of Sentinel-1, Sentinel-2 and Landsat 8 data for Germany," *Remote Sens. Environ.*, vol. 269, Feb. 2022, Art. no. 112831, doi: 10.1016/j.rse.2021.112831.

[4] P. Defourny et al., "Near real-time agriculture monitoring at national scale at parcel resolution: Performance assessment of the Sen2-agri automated system in various cropping systems around the world," *Remote Sens. Environ.*, vol. 221, pp. 551–568, Feb. 2019, doi: 10.1016/j.rse.2018.11.007.

[5] R. d'Andrimont, A. Verhegghen, G. Lemoine, P. Kempeneers, M. Meroni, and M. van der Velde, "From parcel to continental scale—A first European crop type map based on Sentinel-1 and Lucas Copernicus in-situ observations," *Remote Sens. Environ.*, vol. 266, Dec. 2021, Art. no. 112708, doi: 10.1016/j.rse.2021.112708.

[6] Y. Zheng et al., "A new attention-based deep metric model for crop type mapping in complex agricultural landscapes using multisource remote sensing data," *Int. J. Appl. Earth Observ. Geoinformation*, vol. 134, Nov. 2024, Art. no. 104204, doi: 10.1016/j.jag.2024.104204.

[7] Y. Wu, Z. Peng, Y. Hu, R. Wang, and T. Xu, "A dual-branch network for crop-type mapping of scattered small agricultural fields in time series remote sensing images," *Remote Sens. Environ.*, vol. 316, Jan. 2025, Art. no. 114497, doi: 10.1016/j.rse.2024.114497.

[8] D. Gackstetter, M. Körner, and K. Yu, "Approaching holistic crop type mapping in Europe through winter vegetation classification and the hierarchical crop and agriculture taxonomy," *Int. J. Appl. Earth Observ. Geoinformation*, vol. 134, Nov. 2024, Art. no. 104159, doi: 10.1016/j.jag.2024.104159.

[9] P. Griffiths, C. Nendel, and P. Hostert, "Intra-annual reflectance composites from Sentinel-2 and Landsat for national-scale crop and land cover mapping," *Remote Sens. Environ.*, vol. 220, pp. 135–151, Jan. 2019, doi: 10.1016/j.rse.2018.10.031.

[10] S. Preidl, M. Lange, and D. Doktor, "Introducing APiC for regionalised land cover mapping on the national scale using sentinel-2A imagery," *Remote Sens. Environ.*, vol. 240, Apr. 2020, Art. no. 111673, doi: 10.1016/j.rse.2020.111673.

[11] A. Qadir, S. Skakun, I. Becker-Reshef, N. Kussul, and A. Shelestov, "Estimation of sunflower planted areas in Ukraine during full-scale Russian invasion: Insights from Sentinel-1 SAR data," *Sci. Remote Sens.*, vol. 10, Dec. 2024, Art. no. 100139, doi: 10.1016/j.srs.2024.100139.

[12] I. Khosravi, A. Safari, S. Homayouni, and H. McNairn, "Enhanced decision tree ensembles for land-cover mapping from fully polarimetric SAR data," *Int. J. Remote Sens.*, vol. 38, no. 23, pp. 7138–7160, Dec. 2017, doi: 10.1080/01431161.2017.1372863.

[13] S. Asam, U. Gessner, R. A. González, M. Wenzl, J. Kriese, and C. Kuenzer, "Mapping crop types of Germany by combining temporal statistical metrics of Sentinel-1 and Sentinel-2 time series with LPIS data," *Remote Sens.*, vol. 14, no. 13, p. 2981, Jun. 2022, doi: 10.3390/rs14132981.

[14] N. Kussul, M. Lavreniuk, S. Skakun, and A. Shelestov, "Deep learning classification of land cover and crop types using remote sensing data," *IEEE Geosci. Remote Sens. Lett.*, vol. 14, no. 5, pp. 778–782, May 2017, doi: 10.1109/LGRS.2017.2681128.

[15] B. Ghassemi et al., "European union crop map 2022: Earth observation's 10-meter dive into Europe's crop tapestry," *Scientific Data*, vol. 11, no. 1, p. 1048, Sep. 2024, doi: 10.1038/s41597-024-03884-y.

[16] A. Orynbaikyzy, U. Gessner, and C. Conrad, "Crop type classification using a combination of optical and radar remote sensing data: A review," *Int. J. Remote Sens.*, vol. 40, no. 17, pp. 6553–6595, Sep. 2019, doi: 10.1080/01431161.2019.1569791.

[17] I. Khosravi and S. K. Alavipanah, "A random forest-based framework for crop mapping using temporal, spectral, textural and polarimetric observations," *Int. J. Remote Sens.*, vol. 40, no. 18, pp. 7221–7251, Sep. 2019, doi: 10.1080/01431161.2019.1601285.

[18] I. Khosravi, "Advancements in crop mapping through remote sensing: A comprehensive review of concept, data sources, and procedures over four decades," *Remote Sens. Applications: Soc. Environ.*, vol. 38, Apr. 2025, Art. no. 101527, doi: 10.1016/j.rsase.2025.101527.

[19] L. Breiman, "Random forests," *Mach. Learn.*, vol. 45, pp. 5–32, Jun. 2001, doi: 10.1023/A:1010933404324.

[20] J. Louis et al., "Sentinel-2 SEN2COR: L2A processor for users," in *Proc. ESA Living Planet Symp.*, Prague, Czech Republic, 2016.

[21] S. Qiu, Z. Zhu, and B. He, "Fmask 4.0: Improved cloud and cloud shadow detection in Landsats 4–8 and Sentinel-2 imagery," *Remote Sens. Environ.*, vol. 231, Sep. 2019, Art. no. 111205, doi: 10.1016/j.rse.2019.05.024.

[22] D. Zanaga et al. (2020). *ESA WorldCover 10 M 2020 V100*. [Online]. Available: 10.5281/zenodo.5571936

[23] A. Savitzky and M. J. E. Golay, "Smoothing and differentiation of data by simplified least squares procedures," *Anal. Chem.*, vol. 36, no. 8, pp. 1627–1639, Jul. 1964, doi: 10.1021/ac60214a047.

[24] A. Orynbaikyzy, U. Gessner, B. Mack, and C. Conrad, "Crop type classification using fusion of Sentinel-1 and Sentinel-2 data: Assessing the impact of feature selection, optical data availability, and parcel sizes on the accuracies," *Remote Sens.*, vol. 12, no. 17, p. 2779, Aug. 2020, doi: 10.3390/rs12172779.

[25] A. Huete, K. Didan, T. Miura, E. P. Rodriguez, X. Gao, and L. G. Ferreira, "Overview of the radiometric and biophysical performance of the MODIS vegetation indices," *Remote Sens. Environ.*, vol. 83, nos. 1–2, pp. 195–213, Nov. 2002, doi: 10.1016/s0034-4257(02)00096-2.

[26] (2024). *Sentinel Application Platform–SNAP 8.0.5*. [Online]. Available: https://step.esa.int/main/download/snap-download/

[27] (2024). *Google Earth Pro*. [Online]. Available: https://earth.google.com/intl/earth/

[28] P. Olofsson, G. M. Foody, M. Herold, S. V. Stehman, C. E. Woodcock, and M. A. Wulder, "Good practices for estimating area and assessing accuracy of land change," *Remote Sens. Environ.*, vol. 148, pp. 42–57, May 2014, doi: 10.1016/j.rse.2014.02.015.

[29] C. Pelletier, S. Valero, J. Inglada, N. Champion, and G. Dedieu, "Assessing the robustness of random forests to map land cover with high resolution satellite image time series over large areas," *Remote Sens. Environ.*, vol. 187, pp. 156–168, Dec. 2016, doi: 10.1016/j.rse.2016.10.010.

[30] F. Pedregosa et al., "Scikit-learn: Machine learning in Python," *J. Mach. Learn. Res.*, vol. 12, pp. 2825–2830, Nov. 2011.

[31] *Basis-DLM of Baden-Wuerttemberg, Berlin, Brandenburg, Hamburg, Rhineland-Palatinate, Saarland, Saxony, Saxony-Anhalt, and Thuringia, distributed/copyrighted by LGL-BW, Geoportal Berlin, GeoBasis-DE/LGB, LGV, GeoBasis-DE/LVermGeoRP, GeoBasis DE/LVGL-SL, GeoSN, GeoBasis-DE/LVermGeo ST, and GDI-Th, dl-de/by-2-0*, Stuttgart, Berlin, Potsdam, Hamburg, Koblenz, Saarbrücken, Dresden, Magdeburg, Erfurt, Germany,.

[32] *Basis-DLM of Bavaria, Bremen, Mecklenburg-Western Pomerania, Lower Saxony, and Schleswig-Holstein, Distributed/Copyrighted by, LDBV-BY, Landesamt GeoInformation Bremen, GeoBasis-DE/M-V, GeoBasis-DE/LGLN, and GeoBasis-DE/LVermGeo SH, CC BY 4.0*, München, Bremen, Schwerin, Hannover, Kiel, Germany.

[33] *Basis-DLM of North Rhine-Westphalia and Hesse, distributed/copyrighted by Geobasis NRW, and HBVG*, Köln, Wiesbaden, Germany

[34] OpenStreetMap Contributors. (2024). *OpenStreetMap (OSM)*. [Online]. Available: https://planet.openstreetmap.org

[35] E. Meynen, J. Schmithüsen, J. Gellert, E. Neef, H. Müller-Miny, and H. J. Schultze, *Handbuch der Naturräumlichen Gliederung Deutschlands. Bad Godesberg*, Germany: Bundesanstalt für Landeskunde und Raumforschung, 1962, pp. 1953–1962.